

A New Current Dipole Model Satisfying Current Continuity for Inverse Magnetic Field Source Problems

著者	高木 敏行
journal or publication title	IEEE Transactions on Magnetics
volume	41
number	5
page range	1748-1751
year	2005
URL	http://hdl.handle.net/10097/47899

doi: 10.1109/TMAG.2005.846037

A New Current Dipole Model Satisfying Current Continuity for Inverse Magnetic Field Source Problems

Hisashi Endo¹, *Member, IEEE*, Toshiyuki Takagi¹, *Member, IEEE*, and Yoshifuru Saito², *Member, IEEE*

¹Institute of Fluid Science, Tohoku University, Sendai 980-8577, Japan

²Graduate School of Engineering, Hosei University, Tokyo 184-8584, Japan

A new current dipole model is proposed to estimate magnetic field sources. A set of the current dipoles represents a closed-loop current element, always satisfying current continuity. The target region is filled with the closed-loop current elements to derive a system of equations, then its solution estimates unknown current distribution from given magnetic field data. The generalized vector sampled pattern matching method performs applications of current visualization and coil design in this paper, showing that our model stably yields solutions in spite of row-wise rectangular system of equations.

Index Terms—Current dipoles, generalized vector sampled pattern matching (GVSPM) method, inverse source problems, magnetic field source estimation.

I. INTRODUCTION

INVERSE source problems on magnetic fields have been investigated to search for the field sources from locally measured magnetic fields. An application in medical use is to clarify nerve behaviors from the magnetoencephalography (MEG) data around the human brain [1]–[2]. To address this kind of problem results in solving for the ill-posed problems. One of the approaches to carry out is to employ a linear system of equations [3]. The assumed magnetic field sources in the estimating region derives the linear system of equations

$$\mathbf{Y} = C\mathbf{X} \quad (1)$$

where \mathbf{X} represents the estimated field source distribution as a solution vector with order m ; \mathbf{Y} represents the given/assumed magnetic field as an input vector with order n ; moreover, C is a $n \times m$ rectangular coefficient matrix representing the relation between magnetic fields and field sources. In the case of magnetic field source estimation, we have to evaluate field sources from locally measured field data. This means that the number of solutions m is much greater than that of known data n . Single- and multiple-current dipole models are very popular to express the matrix C as the fundamental elements of magnetic field sources. However, it is difficult to satisfy the current continuity, i.e., the divergence of current density must be identically zero. This often makes unstable as well as physically in-existent solutions due to the ill-posed system of equations.

To overcome this difficulty, this paper proposes a closed-loop current model as integrated current dipoles. A set of analytical solutions of line currents makes a closed-loop as a fundamental element of magnetic field source satisfying the current continuity [4]. The magnetic field in total is expressed by linear combination of field distributions caused from the closed-loop current elements. It intends to utilize two-dimensional (2-D) as well as three-dimensional (3-D) CAD data composed of many

small fragments representing the original geometrical shape with good fidelity. After deriving a linear system of equations from the relation between currents and magnetic fields, the generalized vector sampled pattern matching (GVSPM) method is applied to solve the system of equations. GVSPM is an iterative solution strategy for the ill-posed linear system of equations [5]. This solver employs an objective function evaluating the angle obtained by means of inner product between \mathbf{Y} and $C\mathbf{X}$ in (1), [6]. Thus, it is possible to find the solution \mathbf{X} , where both \mathbf{Y} and $C\mathbf{X}$ take the same direction in linear space.

In this paper, two applications are demonstrated. One is current visualization from measured magnetic field distribution data. The other is coil design, which satisfies required magnetic field distribution. The results reveal that the closed-loop current model stably gives solutions in spite of row-wise rectangular system of equations.

II. CURRENT DIPOLES WITH CURRENT CONTINUITY

A. Closed-Loop Current Model

For the inverse magnetic field source problems, we propose a closed-loop current model derived by line integrated current dipoles. The closed-loop currents subdivide the target region as schematically illustrated in Fig. 1. It is just Ampere's law in the classical electromagnetism. One of the advantages of this approach is that 2-D and 3-D mesh data can be used to make closed-loop currents by connecting common branches since the shape of target region/domain is composed of a set of fragments.

B. Discretization

Let the magnetic field caused by the line current to points P_2 toward P_1 be \mathbf{H}_{12} as shown in Fig. 2, then \mathbf{H}_{12} is obtained by Biot–Savart law

$$\mathbf{H}_{12} = \frac{i_m}{4\pi|\mathbf{s} \times \mathbf{r}_2|^2} \left(\frac{\mathbf{r}_2 \cdot \mathbf{s}}{|\mathbf{r}_2|} - \frac{\mathbf{r}_1 \cdot \mathbf{s}}{|\mathbf{r}_1|} \right) \mathbf{s} \times \mathbf{r}_2 \quad (2)$$

where \mathbf{r}_1 and \mathbf{r}_2 are the position vectors to points P_1 and P_2 toward a reference point P_r , respectively; moreover, \mathbf{s} denotes a

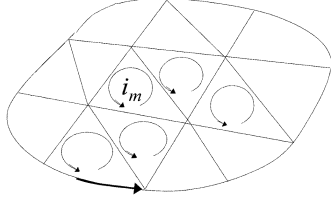


Fig. 1. Closed-loop currents in the target region.

vector indicating current flowing direction. (2) consists of three position vectors so that they are easily calculated from coordinate data in 2-D/3-D mesh system. In the case that the triangular elements are considered, each set of three line currents becomes a magnetic field source. Thereby, the entire magnetic field \mathbf{H} at the reference point P_r is obtained by superposition of three line currents, namely

$$\mathbf{H} = \mathbf{H}_{12} + \mathbf{H}_{23} + \mathbf{H}_{31} \quad (3)$$

where \mathbf{H}_{23} and \mathbf{H}_{31} denote the magnetic fields caused from line currents $P_3 \rightarrow P_2$ and $P_1 \rightarrow P_3$, respectively. In other words, (3) can be summarized in terms of the same current.

C. Current Visualization

Since superposing the magnetic fields caused from every closed-loop current element in the mesh system represents the total magnetic field, then it is possible to obtain a system of equations like (1). The input vector \mathbf{Y} is constructed by the magnetic field intensities in each of measured positions. Therefore, the number of given data n is the product of the number of measured points and number of considered magnetic field components. The solution vector \mathbf{X} is composed of the current intensities of closed-loop current elements. The system matrix C represents the relation between magnetic fields and current intensities by means of (2) and (3).

Solve (1), then the solution vector \mathbf{X} is capable of visualizing/estimating currents. Calculating the sum of currents on a branch makes it possible to show current flowing paths in much the same way as the circuit theory, as illustrated in Fig. 3. In this case, the direction of branch current compulsory determines that of current flow. To derive fine visualization on current flow directions essentially requires an interpolating function on the inside of closed-loop elements. Moreover, to treat linear and non-linear media like magnetic materials a kind of equivalent current source formulation should be studied.

III. GVSPM METHOD

A. System of Equations

Solving the inverse problems results in handling the ill-posed linear system of equations [5]. To solve (1), the present study employs GVSPM method which is an iterative solution strategy for the ill-posed linear system of equations. (1) can be rewritten by

$$\mathbf{Y} = \sum_{i=1}^m x_i \mathbf{C}_i \quad (4)$$

$$\mathbf{X} = [x_1 \ x_2 \ \dots \ x_m]^T, \quad C = [\mathbf{C}_1 \ \mathbf{C}_2 \ \dots \ \mathbf{C}_m]. \quad (5)$$

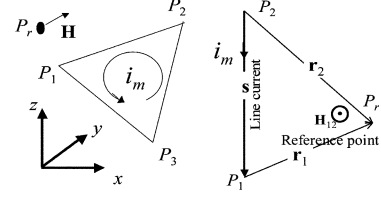
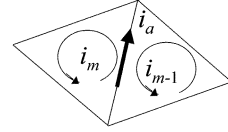

 Fig. 2. Triangular loop current element. Left: Three line currents representing triangular loop current. Right: Calculation of magnetic field caused by the line current from P_2 to P_1 .


Fig. 3. Current flow visualization.

Equation (4) means that the input vector \mathbf{Y} is represented by means of linear combination of column vectors $\mathbf{C}_i, i = 1, 2, \dots, m$, in the system matrix C .

B. Objective Function

Normalizing (4) by vector norm $|\mathbf{Y}|$ gives the following relationship:

$$\frac{\mathbf{Y}}{|\mathbf{Y}|} = \sum_{i=1}^m x_i \frac{|\mathbf{C}_i|}{|\mathbf{Y}|} \frac{\mathbf{C}_i}{|\mathbf{C}_i|} \quad \text{or} \quad \mathbf{Y}' = C' \mathbf{X}' \quad (5)$$

where the prime ($'$) denotes the normalized quantities. Equation (5) means that the normalized input vector \mathbf{Y}' is obtained as a linear combination of the weighted solutions $x_i |\mathbf{C}_i| / |\mathbf{Y}|, i = 1, 2, \dots, m$, with the normalized column vectors $\mathbf{C}_i / |\mathbf{C}_i|, i = 1, 2, \dots, m$. It should be noted that the solution \mathbf{X} could be obtained when an inner product between \mathbf{Y}' and $C' \mathbf{X}'$ becomes 1. This is the key idea of the GVSPM to construct the objective function f derived from the angle between the normalized input and output vectors of the system. When the objective function f in (6) reaches 1, the solution vector \mathbf{X} can be obtained

$$f(\mathbf{X}^{(k)}) = \frac{\mathbf{Y}}{|\mathbf{Y}|} \cdot \frac{C \mathbf{X}^{(k)}}{|C \mathbf{X}^{(k)}|} = \mathbf{Y}' \cdot \frac{C' \mathbf{X}'^{(k)}}{|C' \mathbf{X}'^{(k)}|} \rightarrow 1. \quad (6)$$

C. Iteration Algorithm

Let $\mathbf{X}'^{(0)}$ be an initial solution vector given by

$$\mathbf{X}'^{(0)} = C'^T \mathbf{Y}'. \quad (7)$$

Then, the first deviation vector $\Delta \mathbf{Y}'^{(1)}$ is obtained as

$$\Delta \mathbf{Y}'^{(1)} = \mathbf{Y}' - \frac{C' \mathbf{X}'^{(0)}}{|C' \mathbf{X}'^{(0)}|}. \quad (8)$$

When the deviation $\Delta \mathbf{Y}'$ becomes the zero vector, then (6) is automatically satisfied. Modification by the deviation vector $\Delta \mathbf{Y}'^{(k-1)}$ gives the k -th iterative solution vector $\mathbf{X}'^{(k)}$

$$\begin{aligned} \mathbf{X}'^{(k)} &= \mathbf{X}'^{(k-1)} + C'^T \Delta \mathbf{Y}'^{(k)} \\ &= C'^T \mathbf{Y}' + \left(I_m - \frac{C'^T C'}{|C' \mathbf{X}'^{(k-1)}|} \right) \mathbf{X}'^{(k-1)} \end{aligned} \quad (9)$$

where I_m denotes a m by m unit matrix.

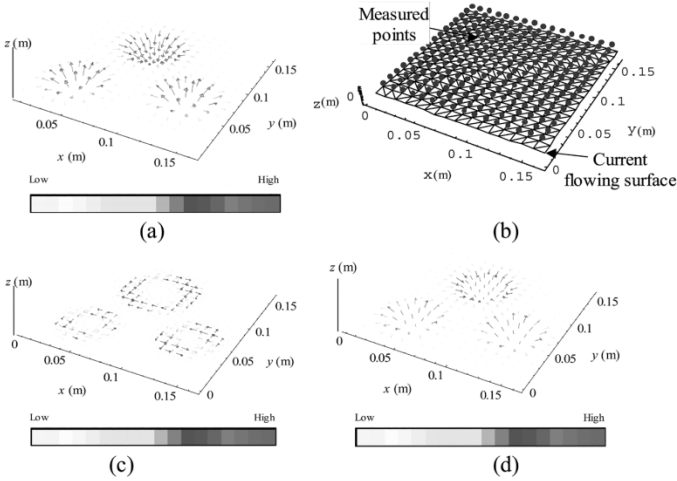


Fig. 4. Current visualization from given magnetic field. (a) Given magnetic field data. (b) Model of analysis. (c) Visualized current vector distribution. (d) Magnetic field reproduced from current shown in (c).

D. Convergence Condition

The convergence condition of the GVSPM iterative strategy is that the modulus of all characteristic values of state transition matrix in (9) must be less than 1. The state transition matrix S is given by

$$S = I_m - \frac{C'^T C'}{|C' \mathbf{X}'^{(k-1)}|} = I_m - \frac{C'^T C'}{|\mathbf{Y}'^{(k-1)}|}. \quad (10)$$

Since the vector $\mathbf{Y}'^{(k-1)}$ is normalized, then (10) can be rewritten by

$$S = I_m - C'^T C'. \quad (11)$$

Let λ be characteristic value of the state transition matrix S . Then, the determinant of symmetrical matrix is obtained

$$|\lambda I_m - S| = \begin{vmatrix} \lambda & \varepsilon_{12} & \cdot & \varepsilon_{1m} \\ \varepsilon_{12} & \lambda & \cdot & \varepsilon_{2m} \\ \cdot & \cdot & \cdot & \cdot \\ \varepsilon_{1m} & \varepsilon_{2m} & \cdot & \lambda \end{vmatrix} = 0. \quad (12)$$

It is obvious that the modulus of off-diagonal elements in (12) take less than 1 because of the normalized column vectors of matrix C' , namely

$$|\varepsilon_{ij}| < 1, \quad i = 1, 2, \dots, m, \quad j = 1, 2, \dots, m. \quad (13)$$

Suppose the modulus characteristic value $|\lambda|$ takes more than 1, then the column vectors in (12) become linear independence because of (13). In such a case, the determinant in (12) is not zero, thus, the condition $|\lambda| < 1$ should be satisfied.

IV. APPLICATIONS

A. Current Visualization

Fig. 4 shows current visualization from magnetic field data. Fig. 4(a) illustrates the given field distribution with 256

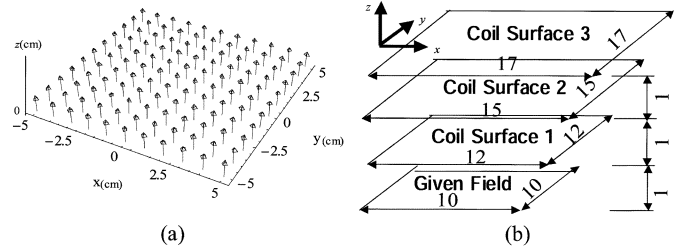


Fig. 5. Problem on coil design. (a) Magnetic field distribution requiring $(H_x, H_y, H_z) = (0, 0, 1)$ A/m. (b) Assumed coil surfaces for exciting coil design. The dimensions shown are in centimeters.

measured points shown in Fig. 4(b). A current flowing surface of $0.16 \times 0.16 \text{ m}^2$ is set up under the measured surface with a distance of 0.01 m. This surface is subdivided by 512 triangular closed-loop current elements. Here, the calculation utilizes z -component of the magnetic field. Therefore, C in (1) is a 256×512 row-wise rectangular matrix. Fig. 4(c) shows estimated current distribution, visualizing three round current loops. About 10 000 GVSPM iterations give the objective function of 1 with allowable error. The computation time is 160.1 s with Mathematica 5.0 on Pentium 4, 2.4-GHz and 1-GB memory machine. Fig. 4(d) shows the reproduced magnetic field from the estimated currents. The correlation coefficient between the original and reproduced fields is 0.9999. Obviously, our model is capable of visualizing current distribution for nondestructive inspection of electronic devices.

B. Coil Design

To demonstrate our approach, we design one of the optimal exciting coil layouts satisfying the desired magnetic field. In Fig. 5, we have homogeneous field in the direction of z axis [$\mathbf{H} = (H_x, H_y, H_z) = (0, 0, 1)$ A/m] on a surface of $10 \times 10 \text{ cm}^2$. The current visualizing approach mentioned in Section IV-A estimates the coil shapes for the desired field.

As shown in Fig. 5(b), we assume three coil surfaces at an interval of 1 cm over the given field surface. Numbers of the triangular elements in coil surfaces 1, 2, and 3 are 288, 450, and 578, respectively. The used magnetic field data consists of the x , y , and z components with 121 points. Since the input vector \mathbf{Y} in (1) has 121×3 elements, then C becomes a 363×1316 row-wise rectangular matrix.

Fig. 6 shows the estimated current distributions obtained from the solution of the 300 000 GVSPM iterations of which objective function (6) reaches 0.99999 as shown in the GVSPM convergence process of Fig. 7. The computation time is 5667.6 s with Mathematica 5.0 on Pentium 4, 2.4-GHz and 1-GB memory machine. The coil surface 3 tends to use high current intensities along with its edges. Moreover, the current intensities at the corners in each coil surface steeply vary to obtain the desired field. Fig. 8 shows the magnetic field distribution reproduced from the current distribution of Fig. 6. The correlation coefficient between the desired and reproduced magnetic fields is 0.99999. In Fig. 8(b), the accuracy of the calculation is shown that the error less than $\pm 2\%$ is performed.

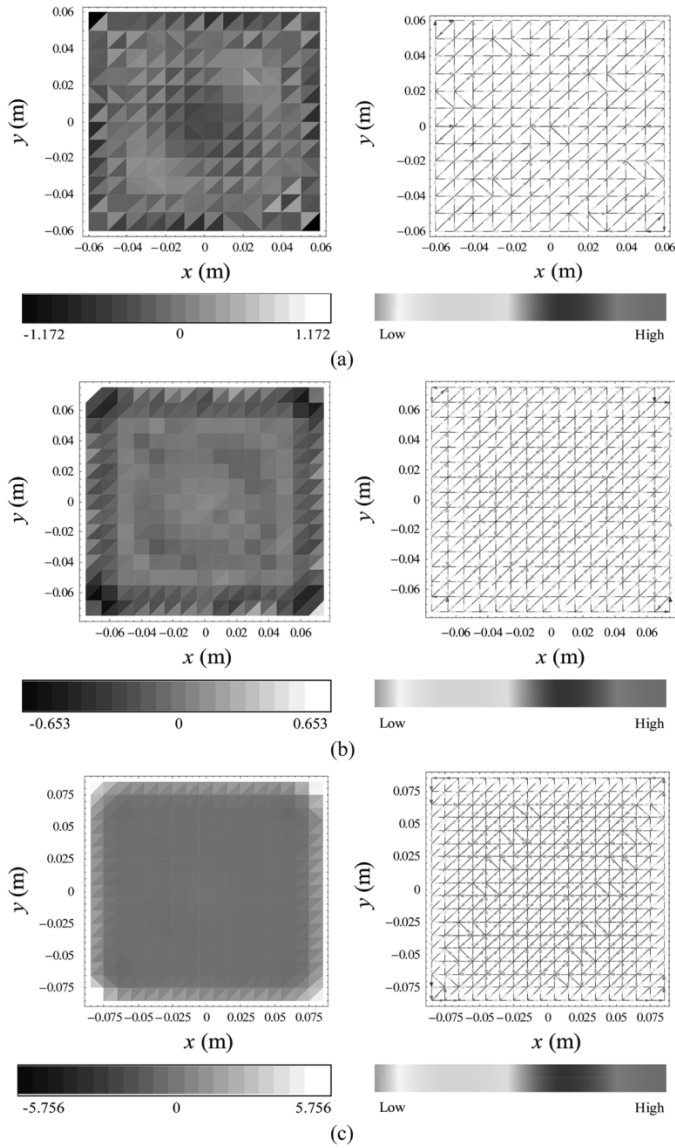


Fig. 6. Evaluated current distributions. (a), (b), and (c) correspond to the results of the coil surface 1, 2, and 3, respectively. Left: Illustration for current intensity in ampere. Right: Current vector visualization.

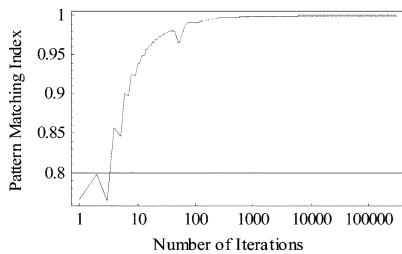


Fig. 7. Convergence process of the GVSPM objective function in (6).

V. CONCLUSION

We have proposed a new current dipole model for the inverse magnetic field source problems. The target region is filled with the closed-loop current elements to satisfy current continuity. The system of equations to estimate currents can be solved by GVSPM stably in spite of row-wise rectangular system matrix.

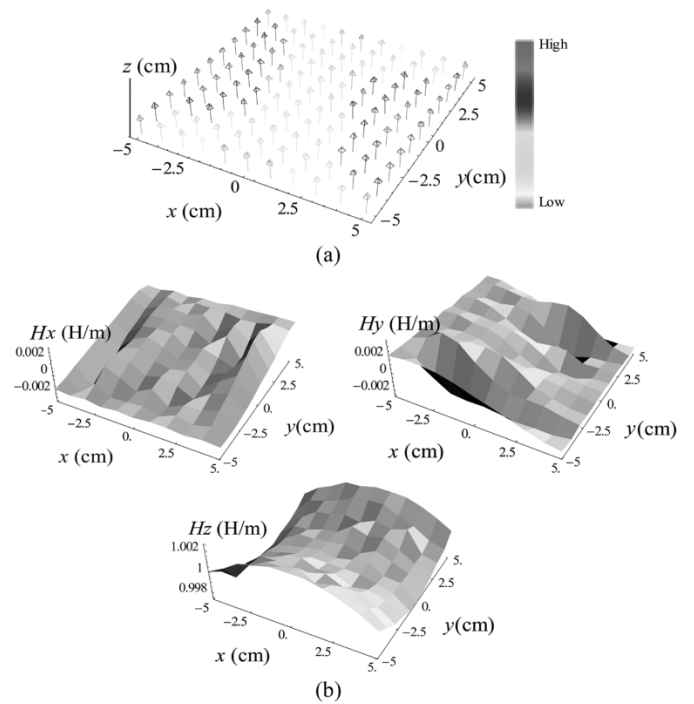


Fig. 8. Reproduced magnetic field distributions. (a) Vector arrow representation. (b) Distribution in each of the magnetic field components.

Because this model always gives physically existing solutions, it enables us to realize the practical magnetic devices. Moreover, it is easy for this approach to employ CAD data with any kind of geometrical elements.

ACKNOWLEDGMENT

This work was supported by a Grant-in-Aid for JSPS Fellows (162972) by the Ministry of Education, Culture, Sports, Science, and Technology, Japan. The authors would like to thank T. Sato of Tohoku University for his helpful advice.

REFERENCES

- [1] Y. Saito, E. Itagaki, and S. Hayano, "A formulation of the inverse problems in magnetostatic fields and its application to a source position searching of the human eye fields," *J. Appl. Phys.*, vol. 67, no. 9, pp. 5830–5832, 1990.
- [2] H. Saotome, K. Kitsuta, S. Hayano, and Y. Saito, "A neural behavior estimation by the generalized correlative analysis," *IEEE Trans. Magn.*, vol. 29, no. 2, pp. 1398–1394, Mar. 1993.
- [3] H. Saotome, K. Kitsuta, S. Hayano, and Y. Saito, "Electromagnetic field source searching from the local field measurement," *Int. J. Appl. Electromagn. Mater.*, vol. 3, pp. 297–306, 1993.
- [4] H. Takahashi, S. Hayano, and Y. Saito, "Visualization of the currents on the printed circuit boards," in *Proc. IEEE Visualization Late Breaking Hot Topics*, San Francisco, CA, 1999, pp. 37–40.
- [5] H. Endo, S. Hayano, Y. Saito, and K. Miya *et al.*, "Generalized vector sampled pattern matching method," in *Studies in Applied Electromagnetics and Mechanics 23 Electromagnetic Nondestructive Evaluation (VI)*, F. Kojima *et al.*, Eds. Amsterdam, The Netherlands: IOS, 2002, pp. 285–292.
- [6] G. Y. Dong, H. Endo, S. Hayano, S. K. Gao, and Y. Saito, "GVSPM for reconstruction in electrical impedance tomography," *IEEE Trans. Magn.*, vol. 39, no. 3, pp. 1630–1633, May 2003.

Manuscript received June 8, 2004.